Supporting Information

Efficient Syngas Production with Controllable CO:H_2 Ratios Based on the Aqueous Electrocatalytic CO_2 Reduction over Mesoporous TiO_2 Films Modified with a Cobalt Porphyrin Molecular Catalyst

Hironobu Ozawa,*[a] Ryoma Kikunaga,[a] Hajime Suzuki,[b] Ryu Abe,[b] and Ken Sakai*[a]

[a] Department of Chemistry, Faculty of Science, Kyushu University, Motooka 744, Nishi-ku, Fukuoka, 819-0395, Japan

[b] Department of Energy and Hydrocarbon Chemistry, Graduate School of Engineering, Kyoto University, Katsura, Nishikyo-ku, Kyoto 615-8510, Japan

Corresponding Author
*E-mail: h.ozawa@chem.kyushu-univ.jp (H.O.)
*E-mail: ksakai@chem.kyushu-univ.jp (K.S.)

Materials and general measurements

Cobalt(II) 5-(4-pyridyl)-10,15,20-triphenylporphyrin (**CoP-py**)[S1,S2] was prepared according to the literature method. All other reagents were purchased from Tokyo Chemical Industry Co., Ltd, and were used without further purification. FTO glasses (PEC-FG01, sheet resistance < 10 Ω, thickness 1.1 mm) were purchased from Peccell Technologies, Inc. TiO_2 paste (PST-18NR) was purchased from JGC Catalysts and Chemicals Ltd.

^{1}H NMR spectra were acquired on a JEOL JNM-ESA 600 spectrometer. ESI-TOF mass spectra were recorded on a JEOL JMS-T100CS spectrometer. ATR-IR spectra were obtained on a Perkin Elmer Spectrum One FT-IR Spectrometer, equipped with a diamond ATR crystal. UV-vis-NIR spectra were recorded on a Shimadzu UV-3600 spectrophotometer. Transmittance and reflectance spectra of the FTO/TiO_2/**CoP-py** electrode was recorded on a Shimadzu UV-3600 spectrophotometer, equipped with an integrated sphere attachment. Cyclic voltammograms (CVs) was recorded on a BAS ALS Model 602DKM electrochemical analyzer, using a glassy carbon working electrode, a platinum wire counter electrode, and an Ag/Ag^+ reference electrode (-0.10 V vs. Fc/Fc^+). The electrolyte solution used was a dimethylformamide containing 0.1 M TBAP (tetra(n-butyl)ammonium perchlorate) as a supporting electrolyte. Scan rate was 100 mV/s. The potentials measured vs. Fc/Fc^+ were converted into those vs. SCE using the value of 0.47 V vs. SCE for Fc/Fc^+ in DMF.[S3] The scanning electron microscopy (SEM) measurements were performed by Hitachi SU8000. The N_2 adsorption and desorption isotherms were measured at liquid nitrogen temperature by using an automatic specific surface area measurement instrument (BELSORP-mini II, MicrotracBEL Corp.). The specific surface area was determined by the Brunauer-Emmett-Teller (BET) method.

Characterization of CoP-Py

ESI-TOF MS (positive ion, CH_3CN) 627.21 m/z ($[\mathbf{M}]^+$). Anal. Calcd. for $C_{43}H_{27}N_5Co \cdot H_2O$ ($[\mathbf{M}] \cdot H_2O$): C, 74.78; H, 4.23; N, 10.14. Found: C, 75.04; H, 4.07; N, 10.13.

Preparation of CoP-py-adsorbed TiO_2 electrodes

Mesoporous TiO_2 thin films on a FTO glass substrate (FTO/TiO_2 electrode) were fabricated by the screen-printing method followed by sintering process.[S2,S4] The apparent size of square-shaped (0.5 cm × 0.5 cm) TiO_2 films are 0.25 cm^2. The film thickness of mesoporous TiO_2 films was measured by a surface profiler (Surfcorder SE300, Kosaka Laboratory Ltd.), and the average film thickness was ca. 12 μm. Modification of a pristine FTO/TiO_2 electrode was performed by submerging it into 0.1 mM **CoP-py** solution of toluene and hexane (3:2, v:v) for 12 h at 20 °C. The amount of **CoP-py** (0.12 μmol/cm^2) adsorbed over the TiO_2 surfaces was spectrophotometrically determined by observing the absorbance change in the immersion bath. After the FTO/TiO_2 electrode was removed from the immersion bath, it was rinsed by a mixed solution of toluene and hexane (3:2, v:v), and dried in vacuo.

Electrochemical measurements for CoP-py-adsorbed TiO_2 electrodes

CV measurements were performed by using a BAS ALS Model 602DKM electrochemical analyzer in a three-electrode configuration electrochemical cell with a **CoP-py**-adsorbed TiO_2 electrode as a working electrode, a carbon rod (6 mmΦ) counter electrode, and an Ag/AgCl reference electrode (-0.01 V vs. SCE). The anodic and cathodic compartments were separated by an anion-exchange membrane (SELEMION, AGC Engineering CO., LTD.). Scan rate was 100 mV/s. The electrolyte solution used was a 0.1 M $NaHCO_3$ solution (pH 8.8). The whole electrochemical cell was degassed with Ar at least 30 min prior to each measurement. For the measurements under CO_2 atmosphere, a 0.1 M $NaHCO_3$ solution was degassed with Ar at least 30 min, followed by CO_2 bubbling at least 30 min. The pH of a CO_2-satrated $NaHCO_3$ buffer solution was 6.8.

Controlled potential electrolysis (CPE) measurements were performed in the same three-electrode configuration electrochemical cell under various applied potentials. The analysis of gases in the headspaces (13.9 cm^2) of both compartments was performed by a Shimadzu GC-14A gas chromatograph equipped with a molecular sieve 13X-S Å column of 2 m × 3 mm i.d. at 30 °C. The injection of the sample gas (200 μL) was performed manually using a gastight syringe. The output signal from the thermal conductivity detector of the gas chromatograph was analyzed using a Shimadzu C-R8A integrator. The CO and H_2 quantities were determined using calibration curves, which have been previously obtained by employing standard CO and H_2 gases. The CPE measurements were performed at least two times to confirm the reproducibility of the results.

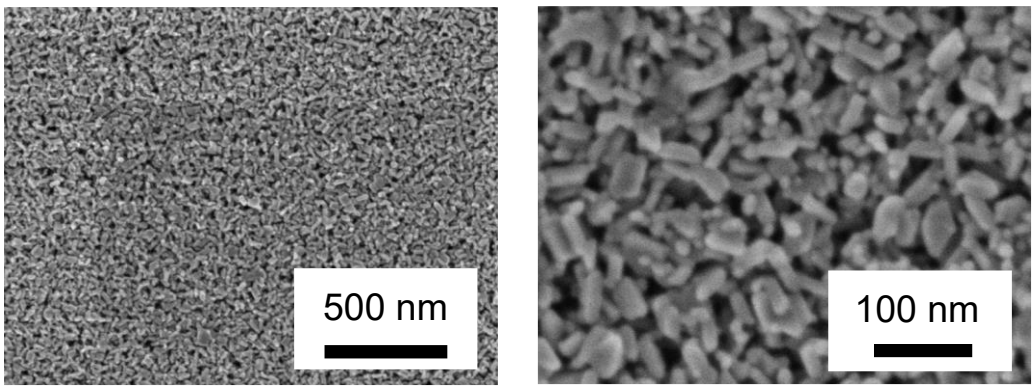

Figure S1. SEM images of the FTO/TiO_2 electrode.

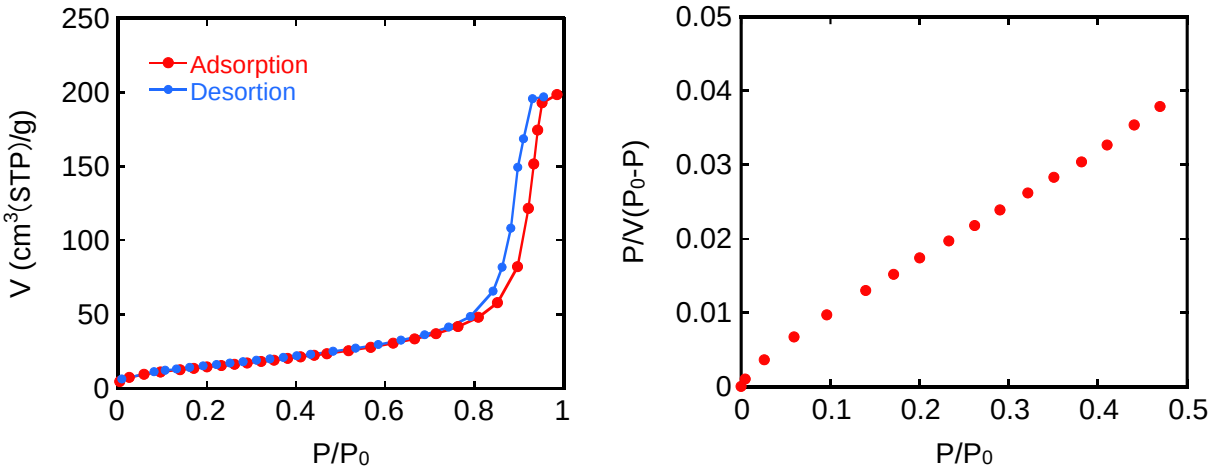

Figure S2. N_2 adsorption and desorption isotherms (left) and BET plot (right) for the mesoporous TiO_2 powder prepared by peeling the TiO_2 thin film off the FTO/TiO_2 electrode.

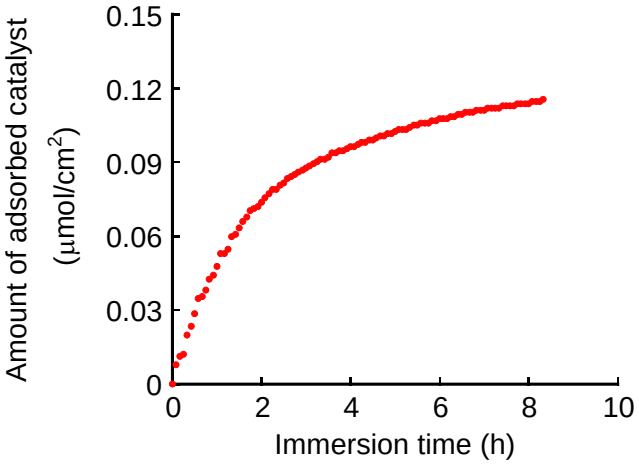

Figure S3. Adsorption profile of **CoP-py** to the mesoporous TiO_2 electrode. Apparent size and the film thickness of mesoporous TiO_2 thin film was 0.25 cm^2 and ca. 12 μm, respectively.

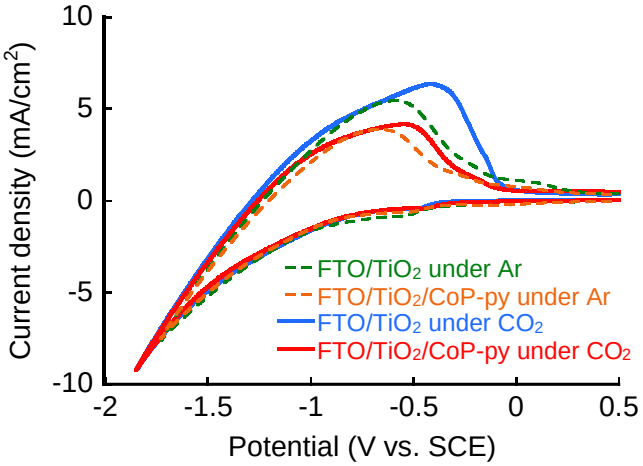

Figure S4. CVs of the FTO/TiO_2 and the FTO/TiO_2/**CoP-py** electrodes in a 0.1 M $NaHCO_3$ solution (pH 8.8) or a CO_2-saturated 0.1 M $NaHCO_3$ solution (pH 6.8). Scan rate was 100 mV/s. The potentials of CVs in 0.1 M $NaHCO_3$ are shifted to the positive direction by 0.12 V, which is the difference between the CB edge potentials at pH 6.8 and 8.8 (-0.92 and -0.80 V vs. SCE, respectively). Apparent size and the film thickness of mesoporous TiO_2 thin film was 0.25 cm^2 and ca. 12 μm, respectively.

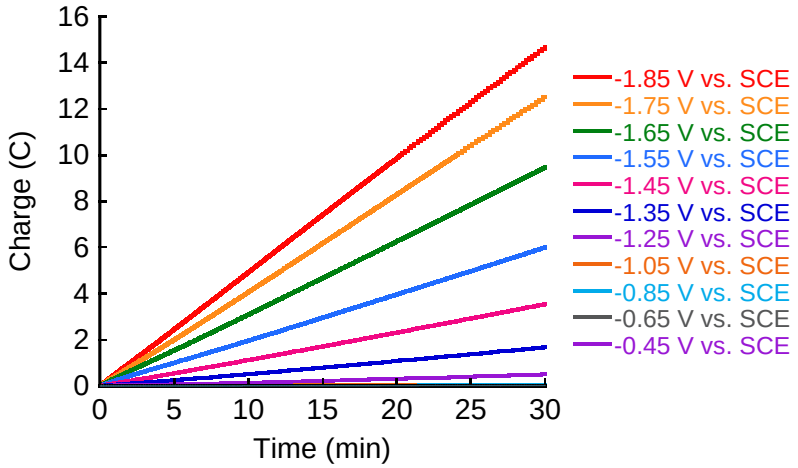

Figure S5. Charge buildup over time during 30 min of CPE for the FTO/TiO_2 electrode under various applied potentials. Apparent size and the film thickness of mesoporous TiO_2 thin film was 0.25 cm^2 and ca. 12 μm, respectively. All measurements were carried out in a three-electrode configuration electrochemical cell with a carbon rod counter electrode and an Ag/AgCl reference electrode in CO_2-saturated 0.1 M $NaHCO_3$ buffer (pH 6.8). These results are raw data for Figure 3 in the main manuscript.

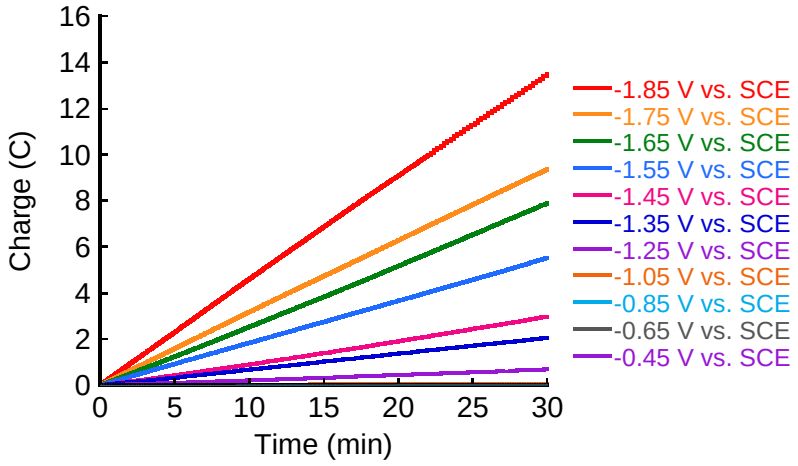

Figure S6. Charge buildup over time during 30 min of CPE for the FTO/TiO_2/**CoP-py** electrode under various applied potentials. Apparent size and the film thickness of mesoporous TiO_2 thin film was 0.25 cm^2 and ca. 12 μm, respectively. All measurements were carried out in a three-electrode configuration electrochemical cell with a carbon rod counter electrode and an Ag/AgCl reference electrode in CO_2-saturated 0.1 M $NaHCO_3$ buffer (pH 6.8). These results are raw data for Figure 3 in the main manuscript.

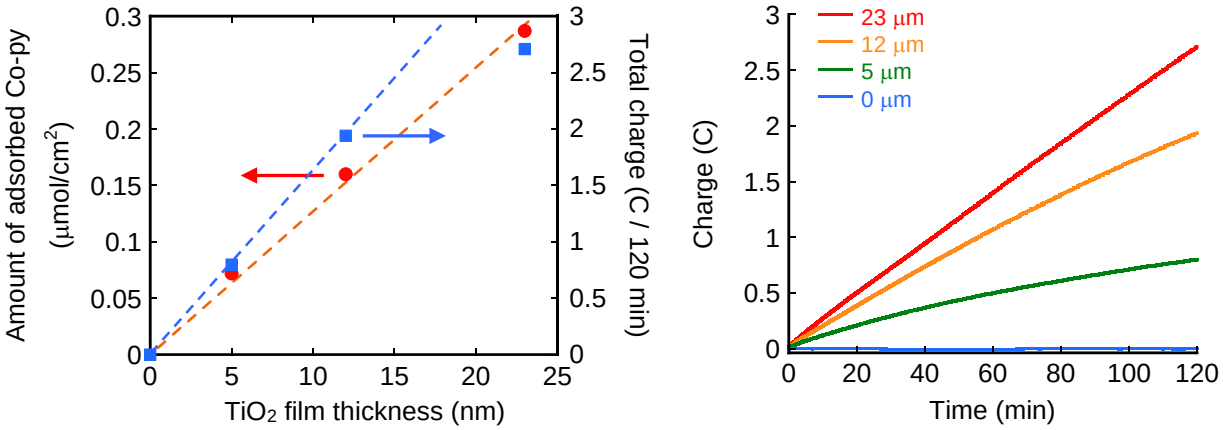

Figure S7. Plots of the amount of adsorbed **CoP-py** and the total charge for 120 min of CPE measurements as a function of the TiO_2 film thickness (left) and charge buildup over time during 120 min of CPE for the FTO/TiO_2/**CoP-py** electrodes with various TiO_2 film thickness in aqueous CO_2-saturated 0.1 M $NaHCO_3$ (pH 6.8) (right). Apparent size of the TiO_2 film was 0.25 cm^2.

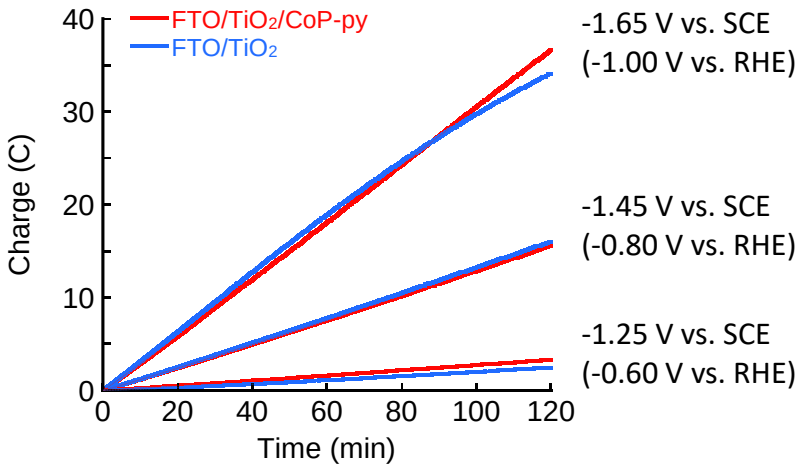

Figure S8. Charge buildup over time during 2 h of CPE for the FTO/TiO_2 and the FTO/TiO_2/**CoP-py** electrodes under the applied potential of -1.25, -1.45, and -1.65 V vs. SCE. Apparent size and the film thickness of mesoporous TiO_2 thin film was 0.25 cm^2 and ca. 12 μm, respectively. All measurements were carried out in a three-electrode configuration electrochemical cell with a carbon rod counter electrode and an Ag/AgCl reference electrode in CO_2-saturated 0.1 M $NaHCO_3$ buffer (pH 6.8). These results are raw data for Figures S9, S10.

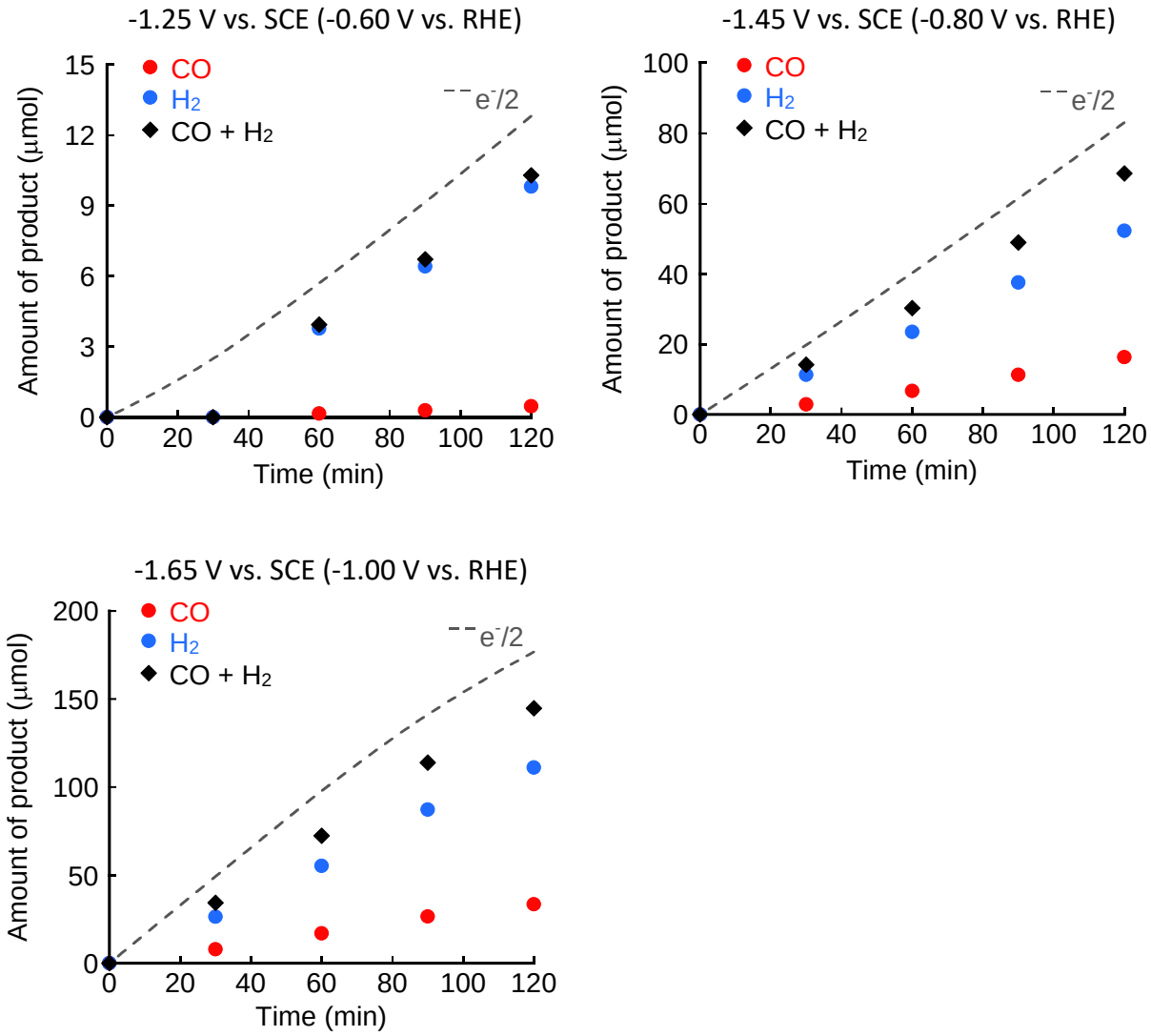

Figure S9. The amounts of CO and H_2 evolved over time during 2 h of CPE for the FTO/TiO_2 electrode at the electrode potential held at -1.25, -1.45, and -1.65 V vs. SCE. Measurements were carried out under the same conditions depicted in Figure S5. The dashed lines correspond to the total amounts of CO and H_2 production with 100% Faradaic efficiency.

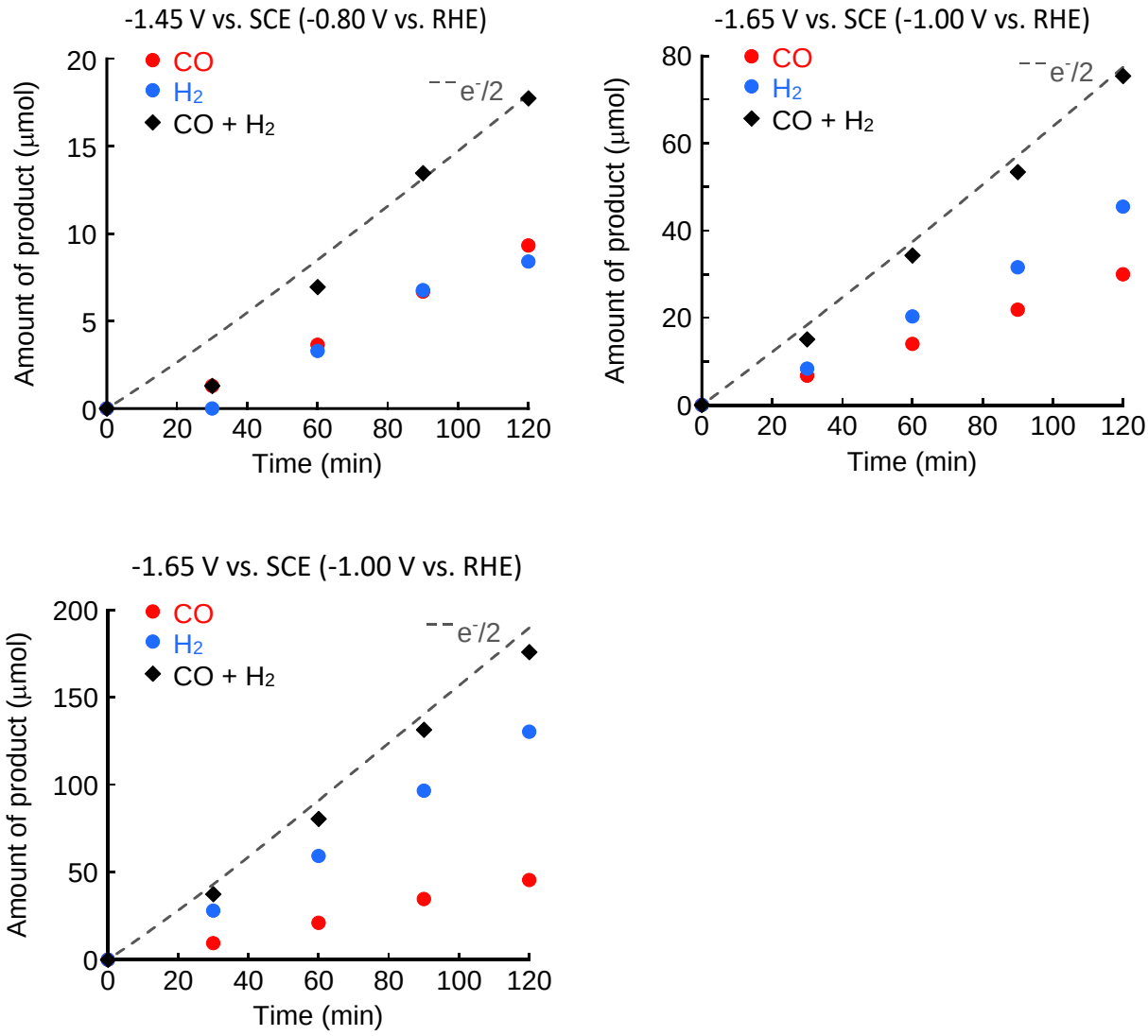

Figure S10. The amounts of CO and H_2 evolved over time during 2 h of CPE for the FTO/TiO_2/**CoP-py** electrode at the electrode potential held at -1.25, -1.45, and -1.65 V vs. SCE. Measurements were carried out under the same conditions depicted in Figure S5. The dashed lines correspond to the total amounts of CO and H_2 production with 100% Faradaic efficiency.

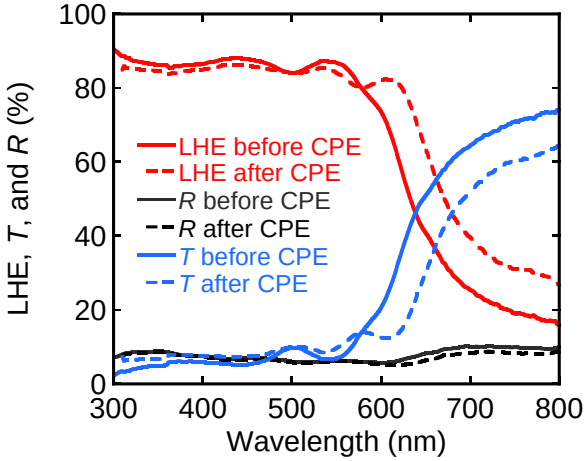

Figure S11. Light harvesting efficiency (LHE) of the FTO/TiO_2/**CoP-py** electrode before and after 2 h of CPE at the applied potential of -1.25 V vs. SCE. LHE was calculated by using the following equation; LHE (%) = 100 – T – R, where T denotes transmittance and R means reflectance.[S5-S7] Note that obvious increase in the LHE after CPE at the wavelength region longer than 580 nm is considered to be attributable to the absorption of the two electron reduced species of **CoP-py** generated during the CPE measurement.

References

S1. B. Steiger, C. Shi, F. C. Anson, *Inorg. Chem.*, **1993**, *32*, 2107-2113.

S2. K. Akamine, K. Morita, K. Sakai, H. Ozawa, *ACS Appl. Energy Mater*., **2020**, *3*, 4860-4866.

S3. N. G. Connelly, W. E. Geiger, *Chem. Rev.* **1996**, *96*, 877-910.

S4. H. Ozawa, T. Sugiura, T. Kuroda, K. Nozawa, H. Arakawa, *J. Mater. Chem. A*, **2016**, *4*, 1762-1770.

S5. K. Sayama, S. Tsukagoshi, T. Mori, K. Hara, Y. Ohga, A. Shinpou, Y. Abe, S. Suga, Suga, H. Suga, *Sol. Energy Mater. Sol. Cells*, **2003**, *80*, 47-71.

S6. M. Liang, W. Xu, F. Cai, P. Chen, B. Peng, J. Chen, Z. Li, *J. Phys. Chem. C*, **2007**, *111*, 4465-4472.

S7. M. Pazoki, U. B. Cappel, E. M. J. Johansson, A. Hagfeldt, G. Boschloo, *Energy Environ. Sci.*, **2017**, *10*, 672-709.